Proceedings of the

FIRST SYMPOSIUM ON ELECTRIC POWER SYSTEMS IN FAST DEVELOPING COUNTRIES

March 21-24, 1987

RIYADH

KINGDOM OF SAUDI ARABIA

SPONSORED BY

KING SAUD UNIVERSITY

IN COOPERATION WITH THE IEEE REGION-8

THE BEHAVIOUR OF H.V. STRAINED CABLES DUE TO SHORT-CIRCUIT CURRENTS

J.L. LILIEN

P. PIROTTE
Senior Member,
IEEE

University of Liege
Belgium

Summary - This paper proposes a calculation method for the flexible components (cables) of H.V. networks (lines, flexible busbars in substation) which are required to operate at a short-circuit current intensity higher than 20 kA.

A simplified model allows an initial fast yet cheap approach. Another model based on the finite element method is able to adjust, when appropriate to a ge extent the options previously taken. erimental full scale tests have confirmed the results obtained by the numerical approach.

The proposed method may include all the components indicated in figure 1.

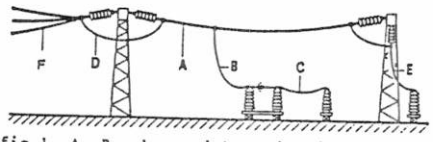

fig.1 A. Bus-bars with string insulators
B. Dropper
C. Connection between apparatus
D. Jumper between two spans
E. Dropper next to structure
F. Dead-end aerial span

1. INTRODUCTION

The magnitude of fault currents continue to increase in power systems. Short circuit currents of 40 to 100 kA are being predicted in the near future (40 kA in Belgium, 63 kA in France, 100 kA in Germany and Canada). Such high currents impose severe equivalent mechanical loads in the system components and also produce large conductor displacements.

The knowledge of the transient mechanical response o complete structure (conductors, insulators, co ctions, supports, ...) is necessary to evaluate firstly the resulting mechanical stresses generated by the applied forces (electromagnetic, gravity, inertial, elastic) and secondly the motion of the cables with the recognition that this may lead to the likelihood of breakdown of the air insulation.

In H.V. substations, the busbars are either rigid or flexible. When the currents distribution is known, the transient response of rigid busbars can be determined using the classical method of linear structures, The case of flexible conductors is a very complex problem that needs non linear theories to take into account the "large displacements" [1],[2],[3],[4]. Moreover, the significant displacement modifies the initial electromagnetic forces and adds a second non-linearity. From the mechanical point of view, due to the very low probability of heavy faults, it is important to know their consequences with sufficient accuracy in order to avoid excessive overdimensionning based on empirical laws.

2. ELECTRICAL CONSIDERATIONS

During fault, the current intensity may be determined by the following simplified expression:

$$i(t) = \sqrt{2}\, I_{rms} \left[\sin(\omega t + \phi) - e^{\frac{-t}{\tau}} \sin\phi\right] \quad (1)$$

where :
- ω angular motion (rad/s)
- τ equivalent time constant of the network at the fault location (s)
- ϕ angle related to the instant when fault appears in accordance with the e.m.f. sine wave of the equivalent network (maximum asymmetry when e.m.f.is zero, that means $\phi = -tg^{-1}(\omega\tau)$(rad)

2.1 Influence of the type of fault on the electromagnetic (EM) forces.

Current multiplication appears in the EM forces representation. The influence of phase differences is very important especially for the continuous component. The mechanical eigenfrequencies of cables in electrical installations are relatively low (about one Hertz). From that time, the mechanical response is practically unaffected by high frequencies induced by the electrical parameters. The d.c. component will be fundamental in defining the motion.

The peak value is of secondary importance so far as low frequencies are concerned compared with those between phases. In these circumstances, the phase-to-phase fault isolated from ground or the three phase fault outer phase will be the most severe in general.

In fact, it is only in these two situations that the force is one-way (fig.2). The figure 3, from tests performed in Czechoslovakia [5], shows the continuous component effect in a three-phase situation. The centre phase is not affected by the force and remains undisturbed. Taking into account this particular effect, the electrical stresses (i.e. the distance between phases) will be more important with the two-phase fault.

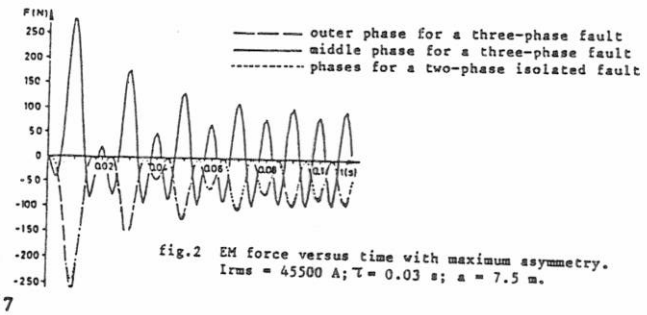

fig.2 EM force versus time with maximum asymmetry.
Irms = 45500 A; τ = 0.03 s; a = 7.5 m.

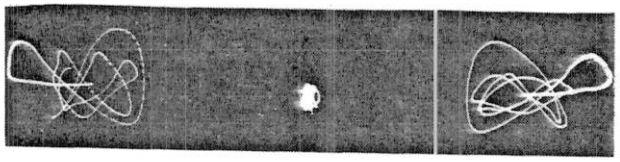

fig.3 Cable oscillations at mid-span for a three-phase fault. A = 1340 mm^2; a = 2.5 M; Irms = 39000 A; t_{c-c} = 0.9 s; T_o = 11800 N; S = 40 m.

In the bundle configuration, as clashing occurs during the 10 to 80 ms following the short-circuit [6], the snatch effect will be more important on the centre phase during a three phase fault if Z_o (Zero Sequence impedance) is greater than Z_d (direct impedance). In other cases (where Z_d is higher than Z_o) the phase-to-ground fault becomes more serious [2].

2.2 Definition of an equivalent intensity in the phase-to-phase isolated fault.

Regarding the importance of the continuous component as discussed previously, we can define the following quantity

$$i(t) = \sqrt{2}\, I_{rms} \sqrt{\frac{1}{2} + e^{-2t/\tau} \sin^2\phi} \qquad (2)$$

which, in the phase-to-phase isolated case, characterizes the equivalent current intensity that determines the continuous component of the force. This process permits a considerable gain in the choice of time integration step for the transient response.

3. MECHANICAL CONSIDERATIONS

It is necessary to take into consideration in the computation of large displacements of the cables, the elasticity and inertia of the cables and their anchoring structures (gantry, towers, insulator supports, ...), conductor heating, gravity and wind, and possible droppers (towards apparatus, ...) and insulator chains (rigid or semi rigid), concentrated masses (pantograph isolator mechanism, ...), and eventually counterpoise mechanisms, cables of various sizes, electromagnetic force variations caused by the movement (Laplace's law), phase-to-phase or three phase faults and a realistic assessment of current flow.

The flexional and torsional stiffnesses of cables may be neglected as these parameters have a very low influence on the phenomenon owing to the magnitude, the direction and the type of the applied forces. Moreover it is difficult to obtain realistic experimental data for them.

Internal and external damping may also be neglected as these values have a small effect upon the maximum values of the response which occurs generally during the first two oscillation periods. These damping coefficients are also very difficult to obtain.

Finally, no account is taken of the possible clash between conductors. We cannot therefore evaluate the snatch effect which takes place when in a bundle conductors are clashing. However this phenomenon only changes the behaviour of the phase during the first moments and the proposed method remains valid for the following motion. We shall return to this problem in our conclusions.

4. FLEXIBLE CABLES ELASTODYNAMIC.[2],[7]

We have chosen the so called fully Lagrangian approach (reference to the structure without strain(initial configuration) at any instant rather than reference to the previous instant). The solution of the system equations is obtained first by taking discrete spatial elements in high order isoparametric finite elements and second by taking discrete time elements using step by step direct integration methods.

4.1 Variational formulation of the motion equations.

Hamilton's principle provides that in a conservative system undergoing displacement variations δu_i kinetically admissible and in such a way $\delta u_i = 0$ at times $t=t_1$ and t_2, the lagrangian action is stationary regarding the real trajectory of the system. We add the electrodynamic forces virtual work (non conservative) to obtain:

$$\delta \int_{t_1}^{t_2} (T-U)dt + \int_{t_1}^{t_2} dt \int_0^{\ell_0} \sum_i^{NC} f_i \cdot \delta u_i \, ds_0 = 0 \qquad (3)$$

where T : cable kinetic energy
U : total potential energy : $U=U_1+U_2$

with U_1 : cable strain energy
U_2 : external conservative loads potential energy (gravity, ...)
l_o : cable length without strain

These definitions are explained in the appendix. Carrying out the variation of expressions taken again in appendix, the equation (3) becomes the virtual work expression that can be applied to transient problems:

$$\int_0^{\ell_0} [(-\rho_0 A_0 \ddot{U}_i + f_i^C + f_i^{NC}) \delta u_i - N \delta g] \, ds_0 = 0 \qquad (4)$$

Where δ_g is the variation of the Green's measure (strain state) and N the tensile force in the cable.

4.2 Spatial Discretisation.[2],[7],[8]

The spatial discretisation of eq. (4) enables a limited number of degrees of freedom of the structure : the nodal unknown (3 displacements) or "generalized displacements".

The structure is cut into finite dimensioned elements. Each finite element must have a simple behaviour in order that the displacement field on one element may be approximated in each direction by a polynomial function guided by the element nodal unknown. The more this function has a higher degree, the more the element is a reasonable representation of a large cable segment (the degree is of course imposed by the number of element nodes : degree 1 for 2 nodes, degree 2 for 3 nodes, ...). An optimum exists between the element degree and the computing time for a constant and satisfactory degree of accuracy in the results.

The discretization is made at the element level, the structure assembling is obtained by expressing the displacement compatibility at the junction nodes, following the assumptions.

The technique uses isoparametric elements : displacements and coordinates are related to the generalized quantities (nodal values) by the same shape functions :

$$u(\xi) = P(\xi).q \qquad (5)$$

and

$$x(\xi) = P(\xi).w \qquad (6)$$

P is the shape function matrix, q and w the displacements and coordinate generalized vectors. (see appendix).

This choice allows an easy union of adjacent elements. The integrals are calculated by numerical quadrature by Gauss's method.

After some development the classical matricial equation for the discretized form of the dynamic equilibrium is obtained :

$$M\ddot{q} = G_{ext} - G_{int} \tag{7}$$

Where M is the (consistent) mass matrix. G_{int} is a non linear function of the generalized displacements q. The solution of (7) needs generally an iterative procedure owing to the high non-linearities of the phenomena. Also by series development we can establish this incremental formulation :

Put down $$r(q_k) = M\ddot{q}_k + G_{int} - G_{ext} \tag{8}$$

Where k characterizes the iteration within a time step and r the residual vector of the forces called "out of balance". G_{int} and G_{ext} are evaluated in function of q_k

$$r(q_{k+1}) = r(q_k) + IT.(q_{k+1} - q_k) = 0 \tag{9}$$

Which may be written

$$IT.\Delta q = - r(q_k) \tag{9'}$$

and also (see appendix)

$$\left[\frac{1}{\zeta h^2} M + K_T\right] . \Delta q = - r(q_k) \tag{10}$$

where h is the time step, ζ a functional parameter of the temporal integration scheme, M the mass matrix and K_T the tangent stiffness matrix.

4.3 Temporal discretization.[2].[9],[10],[11]

We utilize the Newmark's formulations :

$$\dot{q}_{n+1} = \dot{q}_n + (1-\gamma)h\ddot{q}_n + \gamma h\ddot{q}_{n+1} \tag{11}$$

$$q_{n+1} = q_n + h\dot{q}_n + \frac{1}{2}h^2\ddot{q}_n + \beta h^2(\ddot{q}_{n+1} - \ddot{q}_n) \tag{12}$$

With the particular choice of β and γ :

$$\beta = (1-\alpha)^2/4 \tag{13}$$

$$\gamma = \frac{1}{2} - \alpha \tag{14}$$

where $\alpha<0$ assures an unconditionally stable scheme (i.e. independent of the time step h). This scheme introduces a distortion in the frequency response and an artificial damping which may be determined for each system pulsation.

We recommended for α values between -0.1 and -0.3 for the cases studied in this paper. These values have a very small damping effect for low frequencies and the damping of the high frequencies is very favourable for the numerical stability (limitation of round-off errors). We have opted for this scheme because of this.

With the proposed scheme, in the equation (10) ζ is equal to :

$$\zeta = \frac{(1-\alpha)^2}{4} = \beta \tag{15}$$

Remark : the computation strategy will be guided by user experience. It is established that 0.1 sec computing time will be required for each time step for one degree of freedom (and computing time is about proportional to the number of degree of freedom) on IBM 370/158 or VAX 11/780 or also DEC 2050. For the type of problem concerned, the time step chosen is 0.01 sec.[2].

5. COMPARISON BETWEEN CALCULATIONS AND TESTS. [1],[2],[12],[13]

5.1 Example 1 (fig 4 to 11)

The structure tested by LABORELEC (*) represents a 150 kV Belgian substation, see fig. 4. We have taken into account during the computation the stiffness and inertia of the anchoring structures (discretized by classical beam finite elements) and also the droppers connecting the apparatus at ground level.

The discretized structure contains 270 degree of freedom. The fig. 5 to 11 show the test results (continuous line) and the computed results (dashed line) on the same scale.

The comparison is very encouraging. A first maximum occurs at about 0.4 sec. ("swing out") and the second maximum about 1.3 sec ("falling down"). The maximum stress in the dropper (towards 0.3 sec.) is in relationship to the phase conductor which bends the dropper when the distance between two anchoring points becomes equal to its length.

These stresses vary considerably being a function of the problem examined. In the related case, the maximum value of the stress in the cable busbar does not exceed three times the initial value but the short circuit level was limited to 30 kA.

5.2 Example 2 (fig 12 to 14)

With a span similar to that in example 1, the conductor area was 1144 mm^2 (ACSR) and the short circuit current 63 kA (150 kA max) for a duration of 0.242 sec. The supply droppers side is located behind the south gantry; there are no droppers on the north side and the short-circuit was realized with a jumper between the ends of the insulators. The insulator chains were very heavy (300 kg) in relation with real 400 kV substations. Structural stiffness was also greater than in example 1 (by about 10 times) and the first mode of structural oscillation was about 2.5 Hz.

(*) Belgian Laboratory of Electrical Industries.

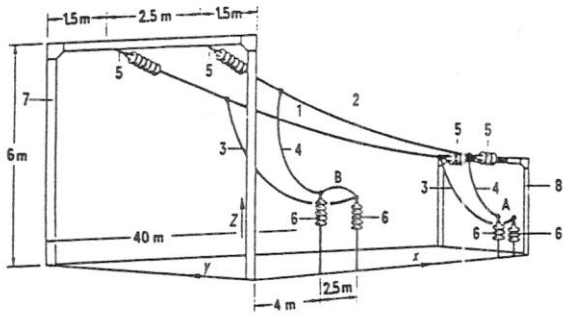

fig.4 exterior switch bay 150kV substation, tested in LABORELEC.
A. current feeding point
B. short-circuit connexion
1...4. 324 mm^2 copper conductor
1. east span (maximum sag 1 m.)
2. west span (maximum sag 1 m.)
3. east dropper, length : 5.6 m.
4. west dropper, length : 4.0 m.
5. arrangement with a length 1.4 m, weight 8 kg, EA = 18000. kN and an insulator chain of length 1.54 m, weight 52.3 kg, EA = 30000.kN.
6. supporting insulators C8-750 (IEC standard) on rigid foundation, height : 2.3 m.
7. north supporting structure
8. south supporting structure
N.B. 1) for 7 and 8 with EURONORM 53-62 :
supports : HE-B260
cross-arms : HE-B240
2) additional masses between cross-arms and supports : 62.2 kg

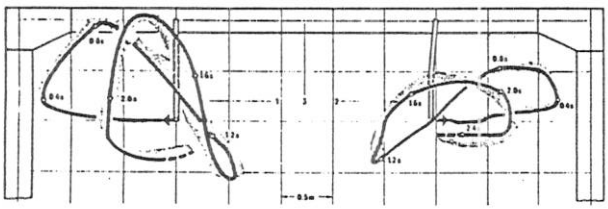

fig.5 Example 1. LABORELEC structure, 30 kA; 0.8 s conductor displacement at mid-span (in a YZ plane)
experimental curves with shadow for range of discrepancy of the numerical results.
1. west cable
2. east cable
3. north supporting structure in the background

fig.6 to 11 comparison between experimental (continuous line) and numerical (dashed line) results with time.

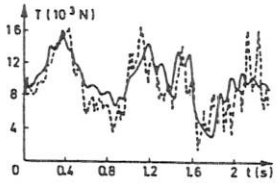

fig.6 east mechanical tension at north anchoring level

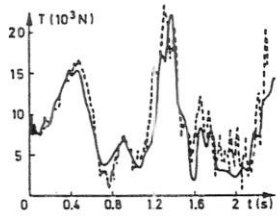

fig.7 west mechanical tension at north anchoring level

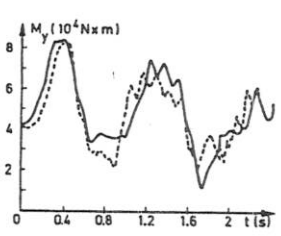

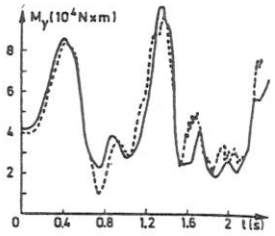

fig.8 bending moment at north-east support, bottom level

fig.9 bending moment at north-west support, bottom level

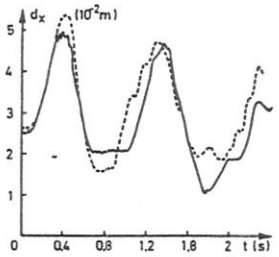

fig.10 displacement of north-east phase anchoring point

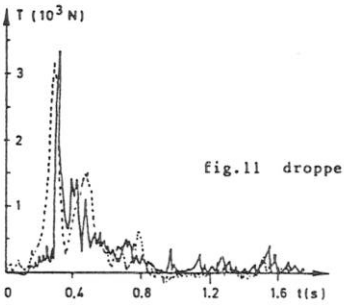

fig.11 dropper mechanical tension

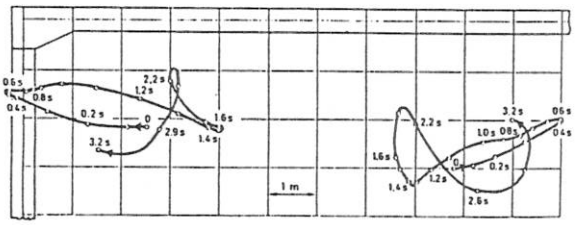

fig.12 Example 2. 63 kA; 0.24 s; 1144 mm^2. Conductor oscillations at mid-span (YZ plane). Similar disposition as in fig. 5.

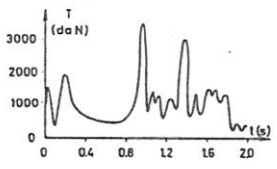

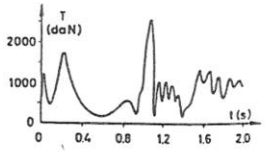

fig.13 Mechanical tension in east cable(sag = 2.2 m)

fig.14 Mechanical tension in west cable (sag = 3.0 m)

The following figures show the evolution of the mid-point of the two phases. The asymmetry may be explained by the difference between initial sags (2.2 and 3 m.). The stress evolution within the phases highlighted an important maximum towards 1 sec, at this moment a perceptible modification in the motion was observed. This phenomenon is related to the frequency excitation of one cable extension ("in plane" motion of the cable) which is about 10 Hz whereas the pendulum oscillation ("out of plane" motion of the cable) is much lower (nearly 0.35 Hz).

5.3 Example 3 (fig 15 and 16)

This example concerns a dead-end span between the line and the substation. The conductor movement in a YZ plane, and hence the evolution of the minimum clearance, is shown in the fig 16. The disposition of the conductors and the imbalance between the anchors provoke a very different motion in the two phases. An important overstress appears in the upper phase during the swinging at about 1 sec.

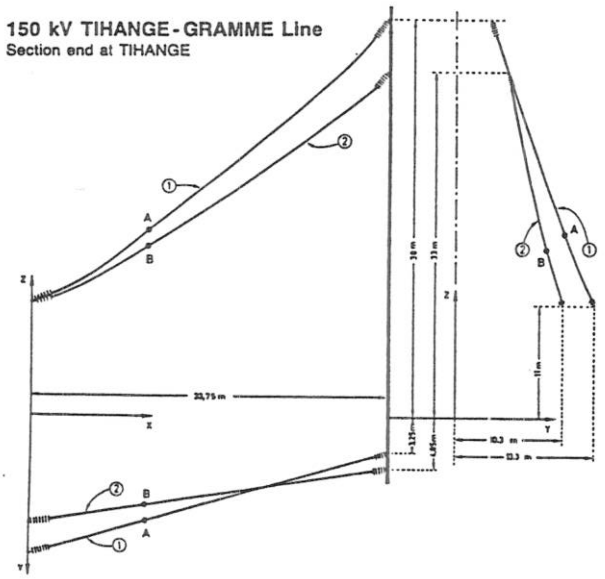

fig.15 Example 3. A 150 kV overhead line. Section end at Tihange. Only the two faulted phases are represented. Points A and B locate the minimum distance between phases.

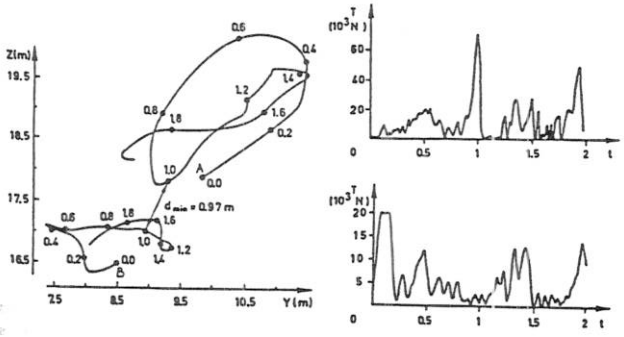

fig.16 conductors oscillations in a YZ plane of points A and B from fig. 15.

6. SIMPLIFIED MODEL. [2], [14]

A very interesting research has been performed by G Ford et al [15]. We would propose a new model, slightly more sophisticated, which takes into account, in a more precise way, the self inertial effect of the insulator chains. Assuming that the shape of the cable remains parabolic, that the anchors are at the same level and that cable points remain coplanar during the motion, it is possible to consider the cable as a two degrees of freedom problem. The insulator is assumed to be inextensible and rigid, its extremity is moving along the circle line of a conical base centered at the anchoring point. One degree of freedom is enough for the insulator model. The anchor stiffness is taken into consideration in the instantaneous evolution of the span length but in order to include the corresponding inertia to take account of the first vibration mode, we can easily add a new degree of freedom. All the forces are assumed to have a uniform distribution on the cable.

The major advantage of this method is the short time required for execution but the model is limited to 3 or 4 degree of freedom i.e. 3 or 4 frequencies. Moreover, this does not take into consideration the jumpers, the exact behaviour of the gantry, the masses which are located at specific points or are non-uniformly distributed. The assumption on the shape is very restrictive and the span has its anchoring points at the same level.

The following figures show the corresponding agreement between the results obtained by the model using the two-armed pendulum and the experimental tests.

6.1 Example 1 (fig 17 and 18)

The agreement is very satisfactory in the case of the west phase but much less for the other phase which has the same behaviour than the west phase when using the pendulum model (which is very different from fig 5 and 6).

The shape no longer corresponds to the assumption when the cable moves downwards, the disagreement increases from this time onwards.

6.2 Example 2 (fig 19 to 21)

It is interesting to note the important influence of the inertia of the insulator chains (see the position of the two arms at the critical moments, the upper arm corresponds to the chain displacements). It can be deduced whether the chains need to be taken into account even in a simplified model. The agreement with

fig.17 and 18
comparison between tests (LABORELEC) and two-arms pendulum

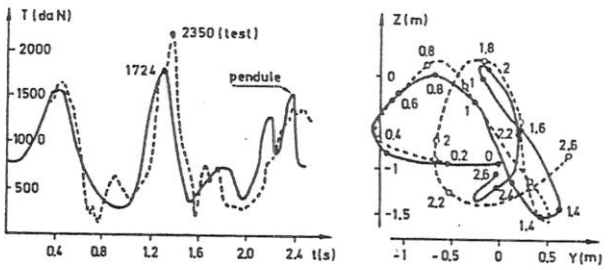

fig.17 mechanical tension in a phase, with time.

fig.18 oscillations of a phase at mid-span, in a YZ plane.

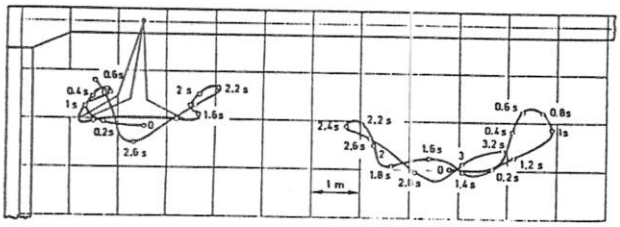

fig.19 oscillations of the two phases at mid-span, in a YZ plane.

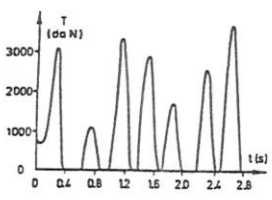

fig.20 mechanical tension in east phase, versus time.

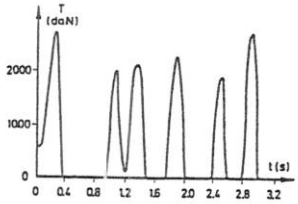

fig.21 mechanical tension in west phase, versus time.

fig 12 to 14 is less good than previously, nevertheless the maximum value is approached very closely. The movement is strongly perturbed, due to interactions between the in plane frequency (about 0.35 Hz) and out of plane frequency (0.56 Hz for phase A and 0.84 Hz for phase B). Resonnance would occur for a factor 2 between those two frequencies. This effect, as seen previously (section 5.2) has less importance due to the large frequency spectrum taken into consideration.

6.3 Example 3

This case is beyond the capability of the simplified model (anchoring points not at the same level, non-uniformity of distributed forces, ...).

7. CONCLUSIONS

In practice it is important to know the behaviour of structures such as substations and lines when faults occur. It is now possible to compute with a good degree of accuracy the behaviour of these types of structures. The following two points must be taken into consideration :

- the mechanical response of structures such as busbars themselves and also connections (droppers, jumpers, ...) to ground mounted apparatus (CT, PT, ...). These values contribute to the mechanical design of the supporting structures.

- the evolution of the distance between cables resulting from the movement which takes place both during and for a period well after the fault. These values contribute to the overall dimensioning of the installation.

We have studied these two types of constraint. The first shows low frequency maximum values (for the busbars) related to the cable movement. With bundle configurations, we must add a high frequency maximum value which appears after the short-circuit occurence. The subsequent behaviour is similar to a single conductor with a mass equal to the total for the bundle. It should be noted that it is convenient to reduce this very specific effect by using an adequate spacer disposition.

From our experience we can confirm that the simplified model (3 or 4 (symmetric case) 6 or 8 (asymmetric case) degrees of freedom) allows a good approach to the problem but the use of this method without interpretation can lead to considerable dimensioning errors.

The combined use of this model with a numerical program taking into account more parameters (inertia of gantry, droppers, complex geometry for the cable, etc...) and less assumptions (type of EM force calculation, etc...) will allow an optimal solution to be obtained which will satisfy the design requirements.

REFERENCES

[1] Lehmann, W., Lilien, J.L., Orkisz, J., The mechanical effects of short-circuit currents in substations with flexible conductors. Numerical methods - computer approach, CIGRE, Session 1982, Rapport 23-08, 1982.

[2] Lilien, J.L., Contraintes et conséquences électromagnétiques liées au passage d'une intensité de courant dans les conducteurs en câble. Collection des publications de la Faculté des Sciences Appliquées, no 87, Université de Liège, Belgique, 1983 (234 références)

[3] Miri, A.M., Heinrich, C., Berechnung des Bewegungsablaufs und des dynamischen Zugkraftverlaufs von gebundelten seilsammelschienen im Kurzschlussfall. Elektrizitatwirtschaft, Jg.82(1983), Heft 9.

[4] Mlodzianowski, A., Waszczyszyn, Z., Analysis of mechanical effects in EHV substations with flexible conductors at short circuit currents. Int. conf. 'Numerical methods for nonlinear problems II' Univ. Barcelona, Spain, 9-13 April 1984.

[5] Cestmir, S., Reimar, V. Personal Communication. Energovod, Prague, 1980.

[6] Manuzio, C., An investigation of forces on bundle conductor spacers under fault conditions, IEEE on PAS, Vol. 86, No 2, pp. 166-184, 1967

[7] Sander, G., Géradin, M., Nysse, C., Hogge, M., Accuracy versus computational efficiency in non-linear dynamics, presented at Fenomech'78 Int. Conf. on Finite Elements in Non-Linear Mechanics, ISD, Universität Stuttgart 30 août-1 sept 1978.

[8] Bathe, K. J., Ramm, E., Wilson, E. L., Finite element formulations for large displacement and large strain analysis, Int. J. Num. Math. Eng. vol. 9, pp. 353-386, 1975.

[9] Key, S. W., Transient response by time integration : review of implicit and explicit operators, Advanced structural dynamics, Ed. J. Donea, Appl. Sc. Publ. London, pp. 71-95, 1980.

[10] Newmark, N. M., A method of computation for structural dynamics, Proc. ASCE. J. Eng. Mech. Div. 85, pp. 67-94, 1959.

[11] Park, K. C., Evaluating time integration methods for non-linear dynamics analysis, ASME, Winter Meeting, Houston, Novembre 1979.

[12] Lilien, J. L., Pirotte, P., Comportement électrodynamique des descentes sur postes en cas de défaut, CIGRE Symposium 22-81, Stockholm, Rapport 112-09, 1981.

[13] Robert, A., Short-circuit tests on flexible busbars. Measurement and calculation of stresses and displacements. Rapport LABORELEC 1-4500/001/E/-JMC/AR, 10 Décembre 1980.

[14] Lilien, J. L., Brokamp, L., Electrodynamic effects due to short-circuit in substations. A two-arms pendulum model, paper CIGRE, 23-84/WG02/04-IWD, March 1984.

[15] Craig, D. B., Ford, G. L., The response of strain bus to short circuit currents, IEEE pas (1980) PP. 434-442, Septembre 1979.

APPENDIX

1. MATHEMATICAL MODEL. KINETIC AND POTENTIAL ENERGIES EXPRESSIONS

$$T = \frac{1}{2}\int_0^{\ell_0} \rho_0 A_0 \sum_i \dot{u}_i^2 \, ds_0 \qquad \text{(A-1)}$$

ρ_o : volumic mass of the unstrained cable (kg/m^3)
A_o : cross section of the unstrained cable (m^2)
$\dot{u}_i$: speed in the i direction of a cable point (m/s)
ds_o : element of unstrained cable length (m)
ℓ_o : unstrained cable length (m)

$U = U_1 + U_2$

$$U_1 = \frac{1}{2}\int_0^{\ell_\rho} \frac{N^2}{EA} ds_o = \frac{1}{2}\int_0^{\ell_0} EA_o \cdot [\, g - \alpha(\theta - \theta_o)\,]^2 \, ds_o \qquad \text{(A-2)}$$

$$U_2 = -\int_0^{\ell_0} \sum_i f_i^c \cdot u_i \, ds_0 \qquad \text{(A-3)}$$

N : axial tension in the cable (N)
EA : extensional stiffness of the unstrained cable (N)
g : measurement of the total strain (elastic and temperature)
we have chosen the Green's measurement of strain which is an exact lagrangian measurement of the strain situation.

$$g = \frac{ds^2 - ds_0^2}{2ds_0^2} \qquad \text{(A-4)}$$

α : linear thermal expansion coefficient (^oC)
$\theta - \theta_o$: the temperature increase (^oC)
f_i : conservative external forces in i-direction (N/m)
u_i : displacement of a cable point in the i-direction from the reference configuration (m)

2. APPLICATION OF DISCRETE FINITE ELEMENTS

Let us write the relations :

$$u(\xi) = P(\xi).q \qquad \text{(A-5)}$$

(displacements)

$$x(\xi) = P(\xi).w \qquad \text{(A-6)}$$

(coordinates)

where q is the generalized displacement vector

w is the generalized coordinate vector for the same nodes
ξ is a normalized variable along the element $[-1,+1]$

The relationship between ds and $d\xi$ is assumed by the jacobian

$$ds_0 = J_0 \, d\xi$$

$$J_0 = \sqrt{\left(\frac{\partial x}{\partial \xi}\right)^2 + \left(\frac{\partial y}{\partial \xi}\right)^2 + \left(\frac{\partial z}{\partial \xi}\right)^2} \qquad \text{(A-7)}$$

P is the shape function matrix.
In the case of the finite element of degree 2 (three nodes) we have :

$$\phi_1 = -\frac{1}{2}\xi \cdot (1-\xi) \qquad \text{(A-8)}$$

$$\phi_2 = \frac{1}{2}\,\xi \cdot (1+\xi) \qquad \text{(A-9)}$$

$$\phi_3 = (1-\xi)\cdot(1+\xi) \qquad \text{(A-10)}$$

$$P(\xi) = \begin{bmatrix} \phi_1(\xi) & 0 & 0 \ldots \phi_n(\xi) & 0 & 0 \\ 0 & \phi_1(\xi) & 0 \ldots 0 & \phi_n(\xi) & 0 \\ 0 & 0 & \phi_1(\xi) \ldots 0 & 0 & \phi_n(\xi) \end{bmatrix} \qquad \text{(A-11)}$$

3. ITERATION MATRIX DEFINITION

$$IT = \frac{\partial r}{\partial q} = M\frac{\partial \ddot{q}}{\partial q} + \frac{\partial Gint}{\partial q} - \frac{\partial Gext}{\partial q} \qquad \text{(A-12)}$$

each term of the iteration matrix is evaluated as a funtion of the displacements at the iteration k

$$\frac{\partial Gint}{\partial q} = K_T \qquad \text{(A-13)}$$

tangential stiffness matrix

$$\frac{\partial Gext}{\partial q} \simeq 0 \qquad \text{(A-14)}$$

because the displacements during a time step are small as are the electromagnetic force variations.

$$\frac{\partial \ddot{q}}{\partial q} = \frac{1}{\zeta h^2} \qquad \text{(A-15)}$$

where h is the time step and is ζ afunction of temporal integration scheme used.

4. ERRORS INTRODUCED BY THE TEMPORAL INTEGRATION SCHEME.

With h the time step, the integration scheme parameter and ω the true pulsation of a structure mode, we can find :

- the critical damping percentage :

$$\xi = \frac{\alpha}{\omega} = \frac{1}{2\omega h} \ln\left[\frac{[4+\omega^2h^2\alpha(1+\alpha)]^2 + 4\omega^2h^2}{[4+\omega^2h^2\alpha(\alpha-1)]^2 + 4\omega^2h^2}\right] \qquad \text{(A-16)}$$

- the frequency distortion :

$$\frac{\Omega}{\omega} = \frac{1}{\omega h} \operatorname{artg}\left|\frac{4\omega h}{4+\omega^2h^2\alpha^2-\omega^2h^2}\right| \qquad \text{(A-17)}$$